ENEA

Ente per le Nuove tecnologie, l'Energia e l'Ambiente

Ministero dello Sviluppo Economico

RICERCA SISTEMA ELETTRICO

Neutronic Methods for Core Calculations of the LFR Innovative Reactor

H. Song, S. Dulla, P. Ravetto

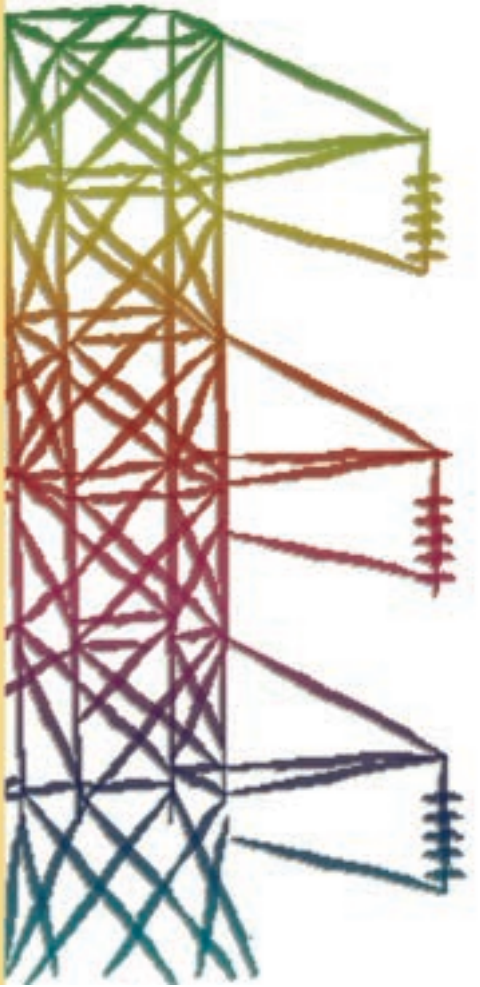

Report RSE/2009/87

Ente per le Nuove tecnologie,
l'Energia e l'Ambiente

Ministero dello Sviluppo Economico

RICERCA SISTEMA ELETTRICO

Neutronic Methods for Core Calculations of the LFR Innovative Reactor

H. Song, S. Dulla, P. Ravetto

Report RSE/2009/87

NEUTRONIC METHODS FOR CORE CALCULATIONS OF THE LFR INNOVATIVE REACTOR

H. Song, S. Dulla, P. Ravetto (CIRTEN)

Dicembre 2008

Report Ricerca Sistema Elettrico
Accordo di Programma Ministero dello Sviluppo Economico – ENEA
Area: Produzione e fonti energetiche
Tema: Nuovo Nucleare da Fissione
Responsabile Tema: Stefano Monti, ENEA

CIRTEN
CONSORZIO INTERUNIVERSITARIO
PER LA RICERCA TECNOLOGICA NUCLEARE

POLITECNICO DI TORINO
DIPARTIMENTO DI ENERGETICA

Neutronic methods for core calculations of the LFR innovative reactor

Metodi neutronici per il calcolo del core del reattore innovativo LFR

Han Song, Sandra Dulla, Piero Ravetto

CIRTEN CERSE-POLITO RL 1253/2008

PISA, DICEMBRE 2008

Lavoro svolto in esecuzione della linea progettuale LP3 punto G dell'AdP ENEA-MSE del 21/06/07 Tema 5.2.5.8 – "Nuovo Nucleare da Fissione".

Neutronic methods for core calculations of the LFR innovative reactor

Han Song, Sandra Dulla and Piero Ravetto

December 17, 2008

Politecnico di Torino
Dipartimento di Energetica
Corso Duca degli Abruzzi, 24 - 10129 Torino (Italy)

ABSTRACT

In the present work a neutronic module for the solution of two-dimensional steady-state multigroup diffusion problems in nuclear reactor cores is developed. The module can produce both direct fluxes as well as adjoint neutron importances. Different numerical schemes are employed. A standard finite-difference approach is firstly implemented, mainly to serve as a reference for less computationally challenging schemes, such as nodal methods and boundary element methods, which are considered in the second part of the work.

The validation of the methods proposed is carried out by comparisons of results for simplified structures. In particular a critical problem for a homogeneous reactor for which an analytical solution exists is considered as a benchmark.

The computational module is then applied to a realistic fast spectrum system, having physical characteristics similar to the proposed lead-cooled ELSY project. The results presented show the effectiveness of the numerical techniques presented. The flexibility and the possibility to obtain neutron importances allow the use of the module for parametric studies, design assessments and integral parameter evaluations, as well as for future sensitivity and perturbation analyses and as a shape solver for time-dependent procedures.

1 Introduction and objective of the work

The European ELSY Project [1] focuses on the assessment of the fast spectrum lead-cooled reactor technology. The physical design of the system requires flexible, efficient and reliable coupled neutronic and thermal-hydraulic tools to carry out extended parametric studies, needed to evaluate and compare the performances of different configurations.

Within this project, a multidimensional neutronic model is being developed both for the steady-state evaluation and as a module for the shape calculations in the quasi-static dynamic

framework for safety assessments. This module is to be coupled with a thermal-hydraulic module to properly account for non-linear effects.

The neutronic module is based on a coarse-mesh approach for the calculation of the neutron distribution of the full core. The present work aims at the evaluation of the performance of different computational schemes, starting from a standard finite volume approach in two-dimensional multigroup diffusion on a fine mesh structure and then proceeding to a nodal formulation of the same problem on a coarse mesh discretization [2]. The inclusion of a computational option based on the boundary element method (BEM) [3, 4] on the same coarse mesh is also under investigation. The interest of such methods is due to the possibility to develop a computational algorithm based on a response matrix formulation, thus allowing an efficient treatment of a full core geometry including the possibility to easily improve the physical model described (i.e., passing from diffusion to transport), retaining the same structure of the numerical code. The comparison of the performances of the two algorithms (nodal and BEM) for the evaluation of the flux distribution in a full core, both in terms of accuracy of prediction and efficiency of calculation, constitutes an important step in the assessment of coarse mesh methods for the application to fast reactors.

The availability of a steady-state flux solver is rather important also for the development of a time-dependent module which is needed for safety evaluations and assessments, within a quasi-static treatment [5]. For that purpose an adjoint solution is also needed. The adjoint can also be used for sensitivity analyses which are rather important for the preliminary design of a new nuclear system.

In a first stage a fine mesh finite difference module in 2D cartesian geometry is developed, as a reference validation tool for coarse mesh and boundary element algorithms. On its turn, such module is validated against analytical results in various configurations.

In a second stage the implementation of a nodal method is carried out. A polynomial representation of the neutron flux within a node is used up to second and third order. Eigenvalue and flux results are reported for different number of meshes. The results show the good performance of the coarse mesh technique associated to a reduced computational effort.

The introduction of a boundary element formulation is then performed and results are presented and compared with previous techniques. The flexibility of the scheme could be of great importance for future application to different configurations of lead-cooled fast reactors.

2 The physical model

The neutronic design of a nuclear reactor core requires the solution of the system of multigroup diffusion equations. The physical characteristics of a lead-cooled reactor call for a multidimensional treatment. In this work the diffusion model is adopted and the equations are solved for a two-dimensional configuration. The neutron steady-state multigroup diffusion

equations without and with an external independent source, respectively, are the following:

$$-\nabla \cdot D^g \nabla \phi_g(\mathrm{r}) + \Sigma_r^g \phi_g(\mathrm{r}) = \sum_{g'=1, g' \neq g}^{G} \Sigma_s^{g' \to g} \phi_{g'}(\mathrm{r}) + \frac{1}{k} \chi^g \sum_{g'=1}^{G} \nu \Sigma_f^{g'} \phi_{g'}(\mathrm{r}), \quad g = 1, 2, \ldots, G \tag{1}$$

and

$$-\nabla D^g \nabla \phi_g(\mathrm{r}) + \Sigma_r^g \phi_g(\mathrm{r}) = \sum_{g'=1, g' \neq g}^{G} \Sigma_s^{g' \to g} \phi_{g'}(\mathrm{r}) + \chi^g \sum_{g'=1}^{G} \nu \Sigma_f^{g'} \phi_{g'}(\mathrm{r}) + s_g(\mathrm{r}), \quad g = 1, 2, \ldots, G, \tag{2}$$

where
D^g - diffusion coefficient of group;
$\Sigma_r^g \equiv \Sigma_a^g + \Sigma_s^g - \Sigma_s^{g \to g}$ - removal cross section of group;
$\Sigma_s^{g \to g'}$ - scattering cross section from group g to group g' ;
$\nu \Sigma_f^{g'}$ - mean number of neutrons per fission times fission cross section of group g';
χ^g - neutron spectrum of group g;
ϕ_g - neutron scalar flux for group g;
s_g - neutron source for group g;
k - effective multiplication constant.
For the homogeneous equation (1) the standard effective multiplication constant is introduced as an eigenvalue, to guarantee solubility.

3 Finite-difference approach

The multigroup diffusion equations without independent source in two dimensional Cartesian coordinate system are considered. The solution of the source-driven problem is derived as one iteration step in the power method used to obtain the eigenvalue. The equations can be written explicitly in the following form:

$$\begin{aligned} &-\frac{\partial}{\partial x} D^g \frac{\partial}{\partial x} \phi_g(x, y) - \frac{\partial}{\partial y} D^g \frac{\partial}{\partial y} \phi_g(x, y) + \Sigma_r^g \phi_g(x, y) \\ &= \sum_{g'=1, g' \neq g}^{G} \Sigma_s^{g' \to g} \phi_{g'}(x, y) + \frac{1}{k} \chi^g \sum_{g'=1}^{G} \nu \Sigma_f^{g'} \phi_{g'}(x, y), \quad g = 1, 2, \ldots, G. \end{aligned} \tag{3}$$

A numerical solution can be obtained by the standard finite difference method, once the domain with $x-$dimension a and $y-$dimension b is subdivided into $I \times J$ meshes which may be chosen as $\Delta_x = a/I$ and $\Delta_y = b/J$. The finite difference solution is used as a reference for the assessment of the coarse-mesh schemes.

By integration over each mesh ($x_{i-\frac{1}{2}} \leq x \leq x_{i+\frac{1}{2}}, y_{j-\frac{1}{2}} \leq y \leq y_{j+\frac{1}{2}}$) one obtains the

following discrete equations:

$$-\frac{D^g_{i-1,j}+D^g_{i-1,j-1}}{2\Delta_x^2}\phi_{g,i-1,j}-\frac{D^g_{i,j}+D^g_{i,-1}}{2\Delta_x^2}\phi_{g,i+1,j}$$

$$-\frac{D^g_{i,j-1}+D^g_{i-1,j-1}}{2\Delta_y^2}\phi_{g,i,j-1}-\frac{D^g_{i-1,j}+D^g_{i,j}}{2\Delta_y^2}\phi_{g,i,j+1}+\left(\bar{\Sigma}^g_{r,i,j}+\frac{2\bar{D}^g_{i,j}}{\Delta_x^2}+\frac{2\bar{D}^g_{i,j}}{\Delta_y^2}\right)\phi_{g,i,j}$$

$$=\sum_{g'=1,g'\neq g}^{G}\bar{\Sigma}_s^{g'\to g}\phi_{g',i,j}+\frac{1}{k}\chi^g\sum_{g'=1}^{G}\nu\bar{\Sigma}_f^{g'}\phi_{g',i,j},$$

$$i=1,2,\ldots,I-1,\ \ j=1,2,\ldots,J-1,\ \ g=1,2,\ldots,G, \tag{4}$$

where $\phi_{g,i,j}$ is the average flux at point (i,j), $D_{i,j}$, $D_{i-1,j}$, $D_{i-1,j-1}$ and $D_{i,j-1}$ are the values of the diffusion coefficients associated to the volume elements contiguous to the point (i,j) and bar quantities are averaged on the computational volume adopted for the integration of the diffusion equations.

Hence, the set of finite difference equations may be written as

$$\mathrm{A}_g\Phi_g=\mathrm{S}_g,\quad g=1,2,\ldots,G \tag{5}$$

where A_g represents the coefficient matrix for group g. Φ_g and S_g are the flux and fission source vectors, respectively, having the size $P=(I-1)\times(J-1)$.

Boundary conditions must also be imposed, letting either the flux (vacuum) or its derivative (symmetry) to vanish on a given surface.

The iterative scheme to solve the problem is established in the classical way [6], introducing an inner iteration procedure, in which, starting from a guessed fission source and effective multiplication constant, the linear system of equations is solved up to convergence on the spatial and energy group flux distribution. Successively, the fission source and the multiplication constant are updated and a new solution for the flux is obtained (outer iteration). The procedure is repeated up to an assumed convergence criterion, i.e. when the following condition between to successive steps is fulfilled:

$$\left|\frac{k^{(n+1)}-k^{(n)}}{k^{(n)}}\right|\leq\epsilon_{out}. \tag{6}$$

An acceleration procedure may significantly reduce the computational effort. The standard overrelaxation method (SOR) is applied for accelerating the inner iterations.

4 Nodal approach

Nodal methods have proved to be very effective for the accurate solution of reactor core physics problems in nuclear engineering applications. The general principle of nodal dif-

fusion theory methods require to subdivide the reactor core into a relatively small number of regions, or nodes, which present dimensions larger than the physical characteristic length associated to the diffusion process. The detailed flux distribution within each node is approximated by the superposition of a suitable set of spatial functions. The global flux distribution is then determined by the application of a weighted residual technique associated to proper conservation principles and coupling conditions for the nodes. In the following the derivation of the nodal scheme is presented for a general 3D system. The node is defined by its sides Δx, Δy and Δz. For each spatial coordinate a one-dimensional equation is obtained by integration over the transverse coordinates. For instance, by integration over y and z, the following equation is obtained for node n, centered at point (x_n, y_n, z_n), and group g:

$$\frac{d}{dx}\overline{J}^n_{gx}(x) + \frac{1}{\Delta y}L^g_{ny}(x) + \frac{1}{\Delta z}L^g_{nz}(x) + \Sigma^g_{tn}\overline{\phi}^n_{gx}(x)$$

$$= \sum_{g'=1}^{G}\Sigma^{g'\to g}_n\overline{\phi}^n_{g'x}(x) + \frac{1}{k}\chi^g\sum_{g'=1}^{G}\nu\Sigma^{g'}_{fn}\overline{\phi}^n_{g'x}(x), \quad g = 1,\ldots,G, \tag{7}$$

where:

$$\overline{\phi}^n_{gx}(x) \equiv \frac{1}{\Delta y\Delta z}\int_{y_n-\Delta y/2}^{y_n+\Delta y/2}dy\int_{z_n-\Delta z/2}^{z_n+\Delta z/2}dz\phi^n_g(x,y,z) \tag{8}$$

$$\overline{J}^n_{gx}(x) \equiv \frac{1}{\Delta y\Delta z}\int_{y_n-\Delta y/2}^{y_n+\Delta y/2}dy\int_{z_n-\Delta z/2}^{z_n+\Delta z/2}dzJ^n_g(x,y,z) \tag{9}$$

$$L^g_{ny}(x) = \frac{1}{\Delta z}\int_{z_n-\Delta z/2}^{z_n+\Delta z/2}dz\,\mathrm{n}_y\cdot[\mathrm{J}_g(x,\frac{y}{2},z) - \mathrm{J}_g(x,-\frac{y}{2},z)] \tag{10}$$

$$L^g_{nz}(x) = \frac{1}{\Delta y}\int_{y_n-\Delta y/2}^{y_n+\Delta y/2}dy\,\mathrm{n}_z\cdot[\mathrm{J}_g(x,y,\frac{z}{2}) - \mathrm{J}_g(x,y,-\frac{z}{2})] \tag{11}$$

Following a well-assessed nodal procedure [7], [8] the unknown transverse-averaged flux $\overline{\phi}^n_{gx}$ is expressed as a superposition of suitable polynomial functions as:

$$\overline{\phi}^n_{gx}(x) \cong \overline{\phi}^n_g f_0(x) + \sum_{i=1}^{3}a^n_{gxi}f_i(x), \quad x_n - \frac{\Delta x}{2} \le x \le x_n + \frac{\Delta x}{2}. \tag{12}$$

If the polynomials herewith appearing are chosen according to the following formulae:

$$\begin{aligned} f_0(x) &= 1, \\ f_1(x) &= \frac{x}{\Delta x} \equiv \xi, \\ f_2(x) &= 3\xi^2 - \frac{1}{4}, \\ f_3(x) &= 2\xi(\xi - \frac{1}{2})(\xi + \frac{1}{2}), \end{aligned} \tag{13}$$

the coefficient of the zeroth-order terms turns out to play the role of node-averaged flux. Furthermore, since $f_3(x_n \pm \Delta x/2) = 0$, the values of the fluxes at the node boundary can be related to the expansion coefficients by:

$$\begin{aligned} a^n_{gx1} &= \phi^n_{gx+} - \phi^n_{gx-} \\ a^n_{gx2} &= \phi^n_{gx+} + \phi^n_{gx-} - 2\overline{\phi}^n_g. \end{aligned} \tag{14}$$

Outgoing surface currents can also be related to the expansion coefficients and to the incoming currents:

$$(J^n_{gx+})_{out} = -\frac{D^g_n}{\Delta x}(a^n_{gx1} + 3a^n_{gx2} + \frac{1}{2}a^n_{gx3}) + (J^n_{gx+})_{in} \tag{15}$$

$$(J^n_{gx-})_{out} = \frac{D^g_n}{\Delta x}(a^n_{gx1} - 3a^n_{gx2} + \frac{1}{2}a^n_{gx3}) + (J^n_{gx-})_{in} \tag{16}$$

The weighted residual method is now applied for the determination of a relationship involving the unknown coefficients a^n_{gx3}. This can be achieved by spatial integration after the application of the weighting function $\omega^g_p = \xi^{2p+1}$ for any group, p being any positive integer. The following expression is readily obtained:

$$\begin{aligned} &-\frac{12D^g_n}{\Delta x^2}a^n_{gx3} + \Sigma^g_{tn}[a^n_{gx1} + \frac{1}{4}(\frac{2p+3}{2p+5} - 1)a^n_{gx3}] \\ &= (\sum_{g'=1}^{G}\Sigma^{g'\to g}_n + \frac{\chi^g}{k}\sum_{g'=1}^{G}\nu\Sigma^{g'}_{fn})[a^n_{g'x1} + \frac{1}{4}(\frac{2p+3}{2p+5} - 1)a^n_{g'x3}]. \end{aligned} \tag{17}$$

It is worth taking the limit for $p \to \infty$, yielding:

$$-\frac{12D^g_n}{(\Delta x)^2}a^n_{gx3} + \Sigma^g_{tn}a^n_{gx1} = \left(\sum_{g'=1}^{G}\Sigma^{g'\to g}_n + \frac{\chi^g}{k}\sum_{g'=1}^{G}\nu\Sigma^{g'}_{fn}\right)a^n_{g'x1}. \tag{18}$$

The physical meaning of this process has been discussed in previous reference works [7], [8] where the present nodal approach is described in full detail.

Combining Eq. (18) with Eqs. (14-16), a relationship connecting incoming and outgoing partial currents with the average flux is obtained:

$$\begin{aligned} &(J^n_{gx+})_{out}(1 + \frac{\Delta x}{12}\Sigma^g_{tn} + \frac{8}{\Delta x}D^g_n) + (J^n_{gx-})_{out}(-\frac{\Delta x}{12}\Sigma^g_{tn} + \frac{4}{\Delta x}D^g_n) - \frac{6}{\Delta x}D^g_n\overline{\phi}^n_g \\ &= (J^n_{gx+})_{in}(1 - \frac{\Delta x}{12}\Sigma^g_{tn} - \frac{8}{\Delta x}D^g_n) + (J^n_{gx-})_{in}(\frac{\Delta x}{12}\Sigma^g_{tn} - \frac{4}{\Delta x}D^g_n) \\ &+\frac{\Delta x}{24}(\sum_{g'=1}^{G}\Sigma^{g'\to g}_n + \frac{\chi^g}{k}\sum_{g'=1}^{G}\nu\Sigma^{g'}_{fn})a^n_{g'x1} \end{aligned} \tag{19}$$

$$
\begin{aligned}
&(J^n_{gx-})_{out}(1+\frac{\Delta x}{12}\Sigma^g_{tn}+\frac{8}{\Delta x}D^g_n)+(J^n_{gx+})_{out}(-\frac{\Delta x}{12}\Sigma^g_{tn}+\frac{4}{\Delta x}D^g_n)-\frac{6}{\Delta x}\overline{D^g_n\phi_g}^n \\
&=(J^n_{gx-})_{in}(1-\frac{\Delta x}{12}\Sigma^g_{tn}-\frac{8}{\Delta x}D^g_n)+(J^n_{gx+})_{in}(\frac{\Delta x}{12}\Sigma^g_{tn}-\frac{4}{\Delta x}D^g_n) \\
&-\frac{\Delta x}{24}(\sum_{g'=1}^{G}\Sigma^{g'\to g}_n+\frac{\chi^g}{k}\sum_{g'=1}^{G}\nu\Sigma^{g'}_{fn})a^n_{g'x1}.
\end{aligned}
\tag{20}
$$

Alternatively the above formulae can be given the following form:

$$
\begin{aligned}
s_{11}(J^n_{gx-})_{out}+s_{12}(J^n_{gx+})_{out}+s_{13}\overline{\phi}^n_g &= s_{14}(J^n_{gx-})_{in}+s_{15}(J^n_{gx+})_{in}+s_{16} \\
s_{12}(J^n_{gx-})_{out}+s_{11}(J^n_{gx+})_{out}+s_{13}\overline{\phi}^n_g &= s_{15}(J^n_{gx-})_{in}+s_{14}(J^n_{gx+})_{in}-s_{16},
\end{aligned}
\tag{21}
$$

where:

$$
\begin{aligned}
&s_{11}=1+\frac{\Delta x}{12}\Sigma^g_{tn}+\frac{8}{\Delta x}D^g_n,\ \ s_{21}=1+\frac{\Delta y}{12}\Sigma^g_{tn}+\frac{8}{\Delta y}D^g_n,\ \ s_{31}=1+\frac{\Delta z}{12}\Sigma^g_{tn}+\frac{8}{\Delta z}D^g_n, \\
&s_{12}=-\frac{\Delta x}{12}\Sigma^g_{tn}+\frac{4}{\Delta x}D^g_n,\ \ s_{22}=-\frac{\Delta y}{12}\Sigma^g_{tn}+\frac{4}{\Delta y}D^g_n,\ \ s_{32}=-\frac{\Delta z}{12}\Sigma^g_{tn}+\frac{4}{\Delta z}D^g_n, \\
&s_{13}=-\frac{6}{\Delta x}D^g_n,\ \ s_{23}=-\frac{6}{\Delta y}D^g_n,\ \ s_{33}=-\frac{6}{\Delta z}D^g_n, \\
&s_{14}=1-\frac{\Delta x}{12}\Sigma^g_{tn}-\frac{8}{\Delta x}D^g_n,\ \ s_{24}=1-\frac{\Delta y}{12}\Sigma^g_{tn}-\frac{8}{\Delta y}D^g_n,\ \ s_{34}=1-\frac{\Delta z}{12}\Sigma^g_{tn}-\frac{8}{\Delta z}D^g_n, \\
&s_{15}=\frac{\Delta x}{12}\Sigma^g_{tn}-\frac{4}{\Delta x}D^g_n,\ \ s_{25}=\frac{\Delta y}{12}\Sigma^g_{tn}-\frac{4}{\Delta y}D^g_n,\ \ s_{35}=\frac{\Delta z}{12}\Sigma^g_{tn}-\frac{4}{\Delta z}D^g_n, \\
&s_{16}=\frac{\Delta x}{24}(\sum_{g'=1}^{G}\Sigma^{g'\to g}_n+\frac{\chi^g}{k}\sum_{g'=1}^{G}\nu\Sigma^{g'}_{fn})a^n_{g'x1}, \\
&s_{26}=\frac{\Delta y}{24}(\sum_{g'=1}^{G}\Sigma^{g'\to g}_n+\frac{\chi^g}{k}\sum_{g'=1}^{G}\nu\Sigma^{g'}_{fn})a^n_{g'x1}, \\
&s_{36}=\frac{\Delta z}{24}(\sum_{g'=1}^{G}\Sigma^{g'\to g}_n+\frac{\chi^g}{k}\sum_{g'=1}^{G}\nu\Sigma^{g'}_{fn})a^n_{g'x1}.
\end{aligned}
\tag{22}
$$

At last, applying the boundary continuity conditions for fluxes and currents, the node balance

equation is cast into the following form:

$$
\begin{aligned}
&\frac{1}{\Delta x}\left\{[(J^n_{gx+})_{out}+(J^n_{gx-})_{out}]-[(J^{n+1}_{gx-})_{out}+(J^{n-1}_{gx+})_{out}]\right\}\\
&+\frac{1}{\Delta y}\left\{[(J^n_{gy+})_{out}+(J^n_{gy-})_{out}]-[(J^{n+1}_{gy-})_{out}+(J^{n-1}_{gy+})_{out}]\right\}\\
&+\frac{1}{\Delta z}\left\{[(J^n_{gz+})_{out}+(J^n_{gz-})_{out}]-[(J^{n+1}_{gz-})_{out}+(J^{n-1}_{gz+})_{out}]\right\}\\
&+\Sigma^g_{tn}\overline{\phi}^n_g=\sum_{g'=1}^{G}\Sigma^{g'\to g}_n\overline{\phi}^n_{g'}+\frac{\chi^g}{k}\sum_{g'=1}^{G}\nu\Sigma^{g'}_{fn}\overline{\phi}^n_{g'},\quad g=1,\ldots,G
\end{aligned}
\tag{23}
$$

At last, equations involving $\overline{\phi}^n_g$, $(J^n_{gx+})_{out}$ and $(J^n_{gx-})_{out}$ for each node are obtained:

$$
\begin{aligned}
(J^n_{gx+})_{out}&=a_1\overline{\phi}^n_g+a_2(J^{n+1}_{gx-})_{out}+a_3(J^{n-1}_{gx+})_{out}+t_1s_{16}\\
(J^n_{gx-})_{out}&=a_4\overline{\phi}^n_g+a_5(J^{n+1}_{gx-})_{out}+a_6(J^{n-1}_{gx+})_{out}-t_1s_{16}\\
(J^n_{gy+})_{out}&=b_1\overline{\phi}^n_g+b_2(J^{n+1}_{gy-})_{out}+b_3(J^{n-1}_{gy+})_{out}+t_2s_{26}\\
(J^n_{gy-})_{out}&=b_4\overline{\phi}^n_g+b_5(J^{n+1}_{gy-})_{out}+b_6(J^{n-1}_{gy+})_{out}-t_2s_{26}\\
(J^n_{gz+})_{out}&=c_1\overline{\phi}^n_g+c_2(J^{n+1}_{gz-})_{out}+c_3(J^{n-1}_{gz+})_{out}+t_3s_{36}\\
(J^n_{gz-})_{out}&=c_4\overline{\phi}^n_g+c_5(J^{n+1}_{gz-})_{out}+c_6(J^{n-1}_{gz+})_{out}-t_3s_{36}\\
\overline{\phi}^n_g&=d_1\overline{S}^n_g+d_2(J^{n+1}_{gx-})_{out}+d_3(J^{n-1}_{gx+})_{out}\\
&\quad+d_4(J^{n+1}_{gy-})_{out}+d_5(J^{n-1}_{gy+})_{out}+d_6(J^{n+1}_{gz-})_{out}+d_7(J^{n-1}_{gz+})_{out},
\end{aligned}
\tag{24}
$$

where:

$$a_1 = a_4 = \frac{(s_{12} - s_{11})s_{13}}{s_{11}^2 - s_{12}^2}, \quad a_2 = a_6 = \frac{s_{11}s_{14} - s_{12}s_{15}}{s_{11}^2 - s_{12}^2}, \quad a_3 = a_5 = \frac{s_{11}s_{15} - s_{12}s_{14}}{s_{11}^2 - s_{12}^2}$$

$$b_1 = b_4 = \frac{(s_{22} - s_{21})s_{23}}{s_{21}^2 - s_{22}^2}, \quad b_2 = b_6 = \frac{s_{21}s_{24} - s_{22}s_{25}}{s_{21}^2 - s_{22}^2}, \quad b_3 = b_5 = \frac{s_{21}s_{25} - s_{22}s_{24}}{s_{21}^2 - s_{22}^2}$$

$$c_1 = c_4 = \frac{(s_{32} - s_{31})s_{33}}{s_{31}^2 - s_{32}^2}, \quad c_2 = c_6 = \frac{s_{31}s_{34} - s_{32}s_{35}}{s_{31}^2 - s_{32}^2}, \quad c_3 = c_5 = \frac{s_{31}s_{35} - s_{32}s_{34}}{s_{31}^2 - s_{32}^2}$$

$$t_1 = \frac{s_{12} + s_{11}}{s_{11}^2 - s_{12}^2}, \quad t_2 = \frac{s_{22} + s_{21}}{s_{21}^2 - s_{22}^2}, \quad t_3 = \frac{s_{32} + s_{31}}{s_{31}^2 - s_{32}^2}$$

$$d_1 = \frac{1}{(\frac{a_1+a_4}{\Delta x} + \frac{b_1+b_4}{\Delta y} + \frac{c_1+c_4}{\Delta z} + \Sigma_{tn}^g)}$$

$$d_2 = (\frac{1 - a_2 - a_5}{\Delta x})d_1, \quad d_3 = (\frac{1 - a_3 - a_6}{\Delta x})d_1$$

$$d_4 = (\frac{1 - b_2 - b_5}{\Delta y})d_1, \quad d_5 = (\frac{1 - b_3 - b_6}{\Delta y})d_1$$

$$d_6 = (\frac{1 - c_2 - c_5}{\Delta z})d_1, \quad d_7 = (\frac{1 - c_3 - c_6}{\Delta z})d_1 \tag{25}$$

The algebraic problem is then solved by standard techniques and outer iterations are carried out for the determination of the multiplication eigenvalue, as discussed above.

5 Boundary Elements approach

The Boundary Elements Method (BEM) [9] constitutes an innovative approach for the solution of diffusion problems in nuclear reactor physics. which are applied to neutron diffusion problems. In previous works the method has been exploited for applications to the solution of multigroup diffusion problems [3, 4]. Also applications to transport problems in space second-order forms have been recently proposed. Results has proven the effectiveness of the technique and its excellent properties [10, 11].

In the following, the basics of boundary element methods for the diffusion problem is outlined. The neutron diffusion equation in a homogeneous region V with a closed smooth boundary surface A is written as:

$$D\nabla_{\mathrm{r}}^2\phi(\mathrm{r}) - \Sigma_a\phi(\mathrm{r}) + q(\mathrm{r}) = 0 \tag{26}$$

The fundamental solution, i.e. the Green function, is found by solving the problem:

$$D\nabla_{\mathrm{r}}^2\tilde{\phi}(\mathrm{r}, \mathrm{r}') - \Sigma_a\tilde{\phi}(\mathrm{r}, \mathrm{r}') + \delta(\mathrm{r} - \mathrm{r}') = 0. \tag{27}$$

Using the properties of the Green function and integrating over the volume Eq. (26), the following integral formulation is obtained:

$$c(\mathrm{r})\phi(\mathrm{r}) + \int_A [\tilde{J}_{\mathrm{n}'}(\mathrm{r},\mathrm{r}'_A)\phi(\mathrm{r}'_A) + \tilde{\phi}(\mathrm{r},\mathrm{r}'_A)J_{\mathrm{n}'}(\mathrm{r}'_A)]dA' = \int_V \tilde{\phi}(\mathrm{r},\mathrm{r}')q(\mathrm{r}')dV', \tag{28}$$

where:

$$\begin{aligned} J_{\mathrm{n}'}(\mathrm{r}'_A) &= -D\frac{\partial\phi(\mathrm{r}'_A)}{\partial \mathrm{n}'_A}, \\ \tilde{J}_{\mathrm{n}'}(\mathrm{r},\mathrm{r}'_A) &= D\frac{\partial\tilde{\phi}(\mathrm{r},\mathrm{r}'_A)}{\partial \mathrm{n}'_A}, \end{aligned} \tag{29}$$

and $c(\mathrm{r})$ is equal to 0, $\frac{1}{2}$ or 1 depending on whether r is outside V, on the boundary of V or inside V, respectively. Eq. (28) allows to obtain $\phi(\mathrm{r})$ and $J_{\mathrm{n}}(\mathrm{r})$ at any point inside V, provided that the flux and the normal current at the points of the boundary surface are known. If we take $\mathrm{r} = \mathrm{r}_A$, Eq. (28) becomes an integral equation

$$c(\mathrm{r}_A)\phi(\mathrm{r}_A) + \int_A [\tilde{J}_{\mathrm{n}'}(\mathrm{r}_A,\mathrm{r}'_A)\phi(\mathrm{r}'_A) + \tilde{\phi}(\mathrm{r}_A,\mathrm{r}'_A)J_{\mathrm{n}'}(\mathrm{r}'_A)]dA' = \int_V \tilde{\phi}(\mathrm{r}_A,\mathrm{r}')q(\mathrm{r}')dV' \tag{30}$$

in terms of the boundary values of ϕ and J_{n}. Introducing the partial currents:

$$\begin{aligned} J^{\pm}_{\mathrm{n}}(\mathrm{r}_A) &= \frac{1}{4}\phi(\mathrm{r}_A) \pm \frac{1}{2}J_{\mathrm{n}}(\mathrm{r}_A) \\ \tilde{J}^{\pm}_{\mathrm{n}}(\mathrm{r}_A) &= \frac{1}{4}\tilde{\phi}(\mathrm{r}_A) \mp \frac{1}{2}\tilde{J}_{\mathrm{n}}(\mathrm{r}_A) \end{aligned} \tag{31}$$

into Eqs.(30), one has

$$\begin{aligned} &\frac{c(\mathrm{r}_A)}{2}J^{+}_{\mathrm{n}}(\mathrm{r}_A) + \int_A \tilde{J}^{+}_{\mathrm{n}'}(\mathrm{r}_A,\mathrm{r}'_A)J^{+}_{\mathrm{n}'}(\mathrm{r}'_A)dA' \\ &= -\frac{c(\mathrm{r}_A)}{2}J^{-}_{\mathrm{n}}(\mathrm{r}_A) + \int_A \tilde{J}^{-}_{\mathrm{n}'}(\mathrm{r}_A,\mathrm{r}'_A)J^{-}_{\mathrm{n}'}(\mathrm{r}'_A)dA' + \frac{1}{4}\int_V \tilde{\phi}(\mathrm{r}_A,\mathrm{r}')q(\mathrm{r}')dV' \end{aligned} \tag{32}$$

Multigroup boundary integral equations. The multigroup equations can be cast in matrix form as:

$$\left(\nabla^2_{\mathrm{r}}\mathrm{I} + \mathrm{Q}\right)\phi(\mathrm{r}) + q(\mathrm{r}) = 0 \tag{33}$$

where ϕ and q are G-dimensional vectors. The definitions of $q(\mathrm{r})$ may be different depending on the presence of an external group source $s_g(\mathrm{r})$. In the case of a subcritical system driven by an external source the following definition holds:

$$q(\mathrm{r}) = s(\mathrm{r}) + \mathrm{F}\phi(\mathrm{r}), \tag{34}$$

where the fission operator takes the form:

$$\mathbf{F} = \begin{pmatrix} (\chi_1/D_1)\nu_1\Sigma_{f1} & (\chi_1/D_1)\nu_2\Sigma_{f2} & \dots & (\chi_1/D_1)\nu_G\Sigma_{fG} \\ (\chi_2/D_2)\nu_1\Sigma_{f1} & (\chi_2/D_2)\nu_2\Sigma_{f2} & \dots & (\chi_2/D_2)\nu_G\Sigma_{fG} \\ \vdots & \vdots & \ddots & \vdots \\ (\chi_G/D_G)\nu_1\Sigma_{f1} & (\chi_G/D_G)\nu_2\Sigma_{f2} & \dots & (\chi_G/D_G)\nu_G\Sigma_{fG} \end{pmatrix}. \tag{35}$$

On the other hand, for the homogeneous problem:

$$q(\mathrm{r}) = \frac{1}{k}\mathrm{F}\phi(\mathrm{r}). \tag{36}$$

The eigenequation

$$\mathrm{Q}\sigma = \lambda\sigma$$

is assumed to have G real distinct eigenvalues λ_h $(h = 1, 2, ..., G)$. S is defined as the matrix which has the normalized eigenvectors σ_h as its columns. Thus, the following equality is verified:

$$\mathrm{S}^{-1}\mathrm{QS} = \Lambda$$

where $\Lambda = \mathrm{diag}[\lambda_1, ..., \lambda_G]$.

Now setting:

$$\phi(\mathrm{r}) = \mathrm{S}\psi(\mathrm{r}),$$

$$q(\mathrm{r}) = \mathrm{S}\eta(\mathrm{r}),$$

after left multiplication by S^{-1}, Eq. (33) reads

$$\nabla^2_{\mathrm{r}}\psi(\mathrm{r}) + \Lambda\psi(\mathrm{r}) + \eta(\mathrm{r}) = 0.$$

By re-defining $\lambda_h = -\gamma_h^2$, the following set of equations is obtained for each component of vector ψ:

$$\nabla^2_{\mathrm{r}}\psi_h(\mathrm{r}) - \gamma_h^2\psi_h(\mathrm{r}) + \eta_h(\mathrm{r}) = 0, \quad h = 1, 2, \dots, G.$$

The corresponding Green fundamental solutions of the following equations

$$\nabla^2_{\mathrm{r},\mathrm{r}'}\tilde{\psi}_h(\mathrm{r},\mathrm{r}') - \gamma_h^2\tilde{\psi}_h(\mathrm{r},\mathrm{r}') + \delta(\mathrm{r}-\mathrm{r}') = 0, \quad h = 1, 2, \dots, G,$$

are easily found out as:

$$\tilde{\psi}_h(\mathrm{r},\mathrm{r}') = \frac{1}{2\pi}K_0(\gamma_h|\mathrm{r}-\mathrm{r}'|),$$

together with their derivatives:

$$\frac{\partial\tilde{\psi}_h(\mathrm{r}'_\Gamma)}{\partial\mathrm{n}'} = \frac{\gamma_h}{2\pi}K_1(\gamma_h|\mathrm{r}-\mathrm{r}'|)\frac{(\mathrm{r}-\mathrm{r}')\cdot\mathrm{n}'}{|\mathrm{r}-\mathrm{r}'|}. \tag{37}$$

Boundary integral equations can be generated with the same procedure leading to Eq. (28), obtaining:

$$c(\mathrm{r})\psi_h(\mathrm{r}) + \int_\Gamma [\frac{\tilde{\psi}_h(\mathrm{r},\mathrm{r}'_\Gamma)}{\partial \mathrm{n}'_\Gamma}\psi_h(\mathrm{r}'_\Gamma) - \tilde{\psi}_h(\mathrm{r},\mathrm{r}'_\Gamma)\frac{\partial\psi_h(\mathrm{r}'_\Gamma)}{\partial \mathrm{n}'_\Gamma}]d\Gamma'$$
$$= \int_\Omega \tilde{\psi}_h(\mathrm{r},\mathrm{r}')\eta_h(\mathrm{r}')d\Omega', \quad h = 1,2,\ldots,G. \tag{38}$$

By left multiplying the set of equations (38) written in matrix form by S, one gets back to relations involving ϕ, namely:

$$c(\mathrm{r})\phi_g(\mathrm{r}) + \sum_{g'=1}^{G}\int_\Gamma [\frac{\tilde{\Psi}_{gg'}(\mathrm{r},\mathrm{r}'_\Gamma)}{\partial \mathrm{n}'_\Gamma}\phi_{g'}(\mathrm{r}'_\Gamma) - \tilde{\Psi}_{gg'}(\mathrm{r},\mathrm{r}'_\Gamma)\frac{\partial\phi_{g'}(\mathrm{r}'_\Gamma)}{\partial \mathrm{n}'_\Gamma}]d\Gamma'$$
$$= \sum_{g'=1}^{G}\int_\Omega \tilde{\Psi}_{gg'}(\mathrm{r},\mathrm{r}')q_{g'}(\mathrm{r}')d\Omega', \quad g = 1,2,\ldots,G, \tag{39}$$

where

$$\tilde{\Psi}_{gg'}(\mathrm{r},\mathrm{r}'_\Gamma) = \sum_{h=1}^{G}\sigma_{gh}\tilde{\psi}_h(\mathrm{r},\mathrm{r}'_\Gamma)\sigma^*_{hg'}. \tag{40}$$

Let r be taken on the boundary, $\mathrm{r} = \mathrm{r}_\Gamma$. Then finally the multigroup boundary integrated equations can be explicitly written down:

$$\frac{c(\mathrm{r}_\Gamma)}{2}J^+_g(\mathrm{r}_\Gamma) + \sum_{g'=1}^{G}\int_\Gamma \tilde{J}^+_{gg'}(\mathrm{r}_\Gamma,\mathrm{r}'_\Gamma)J^+_{g'}(\mathrm{r}'_\Gamma)d\Gamma'$$
$$= -\frac{c(\mathrm{r}_\Gamma)}{2}J^-_g(\mathrm{r}_\Gamma) + \sum_{g'=1}^{G}\int_\Gamma \tilde{J}^-_{gg'}(\mathrm{r}_\Gamma,\mathrm{r}'_\Gamma)J^-_{g'}(\mathrm{r}'_\Gamma)d\Gamma' + \frac{1}{4}\sum_{g'=1}^{G}\int_\Omega \tilde{\Psi}_{gg'}(\mathrm{r}_\Gamma,\mathrm{r}')q_{g'}(\mathrm{r}')d\Omega',$$
$$g = 1,2,\ldots,G, \tag{41}$$

where:

$$J^\pm_g(\mathrm{r}_\Gamma) = \frac{1}{4}\phi(\mathrm{r}_\Gamma) \mp \frac{1}{2}D_g\frac{\partial\phi(\mathrm{r}_\Gamma)}{\partial \mathrm{n}_\Gamma},$$
$$\tilde{J}^\pm_{gg'}(\mathrm{r}_\Gamma,\mathrm{r}'_\Gamma) = \frac{1}{4D_{g'}}\tilde{\Psi}(\mathrm{r}_\Gamma,\mathrm{r}'_\Gamma) \pm \frac{1}{2}\frac{\partial\tilde{\Psi}(\mathrm{r}_\Gamma,\mathrm{r}'_\Gamma)}{\partial \mathrm{n}'_\Gamma}. \tag{42}$$

Reduction of the domain integrals of the source term. The domain integrals involving the independent and flux dependent fission sources in Eqs. (41) can be reduced into a bound-

ary integrated form as:

$$\begin{aligned}
&\int_{\Omega} \tilde{\Psi}_{gg'}(\mathrm{r}_\Gamma, \mathrm{r}') q_{g'}(\mathrm{r}') d\Omega' \\
&= \sum_{h=1}^{G} \frac{-\sigma_{gh}\sigma_{hg'}}{B_h^2} \left\{ c(\mathrm{r}_\Gamma) q_{g'}(\mathrm{r}_\Gamma) + \int_{\Omega} \tilde{\psi}_h(\mathrm{r}_\Gamma, \mathrm{r}') q_{g'}(\mathrm{r}') d\Omega' \right. \\
&\left. + \int_{\Gamma} [\frac{\tilde{\psi}_h(\mathrm{r}_\Gamma, \mathrm{r}'_\Gamma)}{\partial \mathrm{n}'_\Gamma} q_{g'}(\mathrm{r}'_\Gamma) - \tilde{\psi}_h(\mathrm{r}_\Gamma, \mathrm{r}'_\Gamma) \frac{\partial q_{g'}(\mathrm{r}'_\Gamma)}{\partial \mathrm{n}'_\Gamma}] d\Gamma' \right\} \qquad (43) \\
&= \sum_{h=1}^{G} \frac{-\sigma_{gh}\sigma_{hg'}}{B_h^2} \left\{ c(\mathrm{r}_\Gamma) q_{g'}(\mathrm{r}_\Gamma) \right. \\
&\left. + \int_{\Gamma} \left[\frac{\tilde{\psi}_h(\mathrm{r}_\Gamma, \mathrm{r}'_\Gamma)}{\partial \mathrm{n}'_\Gamma} q_{g'}(\mathrm{r}'_\Gamma) - \tilde{\psi}_h(\mathrm{r}_\Gamma, \mathrm{r}'_\Gamma) \frac{\partial q_{g'}(\mathrm{r}'_\Gamma)}{\partial \mathrm{n}'_\Gamma} \right] d\Gamma' \right\}, \quad h = 1, 2, \ldots, G.
\end{aligned}$$

The source distributions $q_g(\mathrm{r})$ are now assumed to be either spatially constant or first-order polynomials. In the latter case for 2D geometry the following expression is assumed:

$$q(x, y) = l_1 x + l_2 y + \bar{q}, \qquad (44)$$

where, obviously, $\bar{q}$ is the average source on the domain. , within the domain $x \in [0, a]$ and $y \in [0, b]$. We have

$$q_{g'}(x, y) = l_1 x + l_2 y + \bar{q}_{g'} - \left(\frac{a l_1}{2} + \frac{b l_2}{2} \right). \qquad (45)$$

As $\bar{q}$ in the presence of fission emissions is evaluated by the flux of the previous generation on the boundary, the coefficients of expansion (44) can be evaluated by using a least-square approach. The problem can be nicely written in matrix form

$$Ml = N, \qquad (46)$$

having set the following definitions:

$$M = \begin{pmatrix} x_1 - \frac{\Delta x}{2} & y_1 - \frac{\Delta y}{2} \\ x_2 - \frac{\Delta x}{2} & y_2 - \frac{\Delta y}{2} \\ \vdots & \vdots \\ x_N - \frac{\Delta x}{2} & y_N - \frac{\Delta y}{2} \end{pmatrix}, l = \begin{pmatrix} l_1 \\ l_2 \end{pmatrix}, N = \begin{pmatrix} q_1 - \bar{q} \\ q_2 - \bar{q} \\ \vdots \\ q_N - \bar{q} \end{pmatrix}, \qquad (47)$$

where (x_i, y_i) are points on the boundary at which the source takes the value q_i. By left multiplication of Eq. (46) by M^T, the normal equations are obtained for the problem:

$$M^T M l = M^T N,$$

or, explicitly:

$$\begin{pmatrix} \sum_{n=1}^{N}(x_n-\frac{a}{2})^2 & \sum_{n=1}^{N}(x_n-\frac{a}{2})(y_n-\frac{b}{2}) \\ \sum_{n=1}^{N}(x_n-\frac{a}{2})(y_n-\frac{b}{2}) & \sum_{n=1}^{N}(y_n-\frac{b}{2})^2 \end{pmatrix} \begin{pmatrix} l_1 \\ l_2 \end{pmatrix} = \begin{pmatrix} \sum_{n=1}^{N}(x_n-\frac{a}{2})(q_{g,n}-\bar{q}_g) \\ \sum_{n=1}^{N}(y_n-\frac{b}{2})(q_{g,n}-\bar{q}_g) \end{pmatrix} \tag{48}$$

The above system of equations yields the value of two-dimensional vector l.

Discretization of the boundary integral equations. In this section the numerical solution of Eqs. (41) is outlined. The boundary Γ is partitioned into I elements of length d_i. After denoting the two extremes and the middle point by $\mathrm{r}_{\Gamma,i-\frac{1}{2}}$, $\mathrm{r}_{\Gamma,i+\frac{1}{2}}$ and $\mathrm{r}_{\Gamma,i}$, respectively, a local dimensionless coordinate τ is introduced to denote each point r along Γ_i as

$$\mathrm{r} = \mathrm{r}_{\Gamma,i} + \tau(\mathrm{r}_{\Gamma,i+\frac{1}{2}} - \mathrm{r}_{\Gamma,i-\frac{1}{2}}). \tag{49}$$

Thus, it is assumed that

$$J_g^{\pm}(\mathrm{r}_\Gamma) = J_{g,i}^{\pm}. \tag{50}$$

Then, assuming a linear behaviour on each boundary mesh of the integrand functions, the boundary integrals are approximated by finite sums as:

$$\begin{aligned} &\int_\Gamma \tilde{J}_{gg'}^{\pm}(\mathrm{r}_{\Gamma,i},\mathrm{r}'_\Gamma) J_{g'}^{\pm}(\mathrm{r}'_\Gamma) d\Gamma' \\ &\cong \sum_{j=1}^{I}\int_{-1}^{1} \tilde{J}_{gg'}^{\pm}\left(\mathrm{r}_{\Gamma,i},\mathrm{r}'_{\Gamma,j}+\tau\left(\mathrm{r}_{\Gamma,j+\frac{1}{2}}-\mathrm{r}_{\Gamma,j-\frac{1}{2}}\right)\right) J_{g',j}^{\pm}\frac{d_j}{2}d\tau. \end{aligned} \tag{51}$$

By indicating

$$q_g(\mathrm{r}_\Gamma) = q_{g,i}, \qquad \frac{\partial q_g(\mathrm{r}_\Gamma)}{\partial \mathrm{n}_\Gamma} = q'_{g,i}. \tag{52}$$

one has:

$$\begin{aligned} &\int_\Gamma \left[\frac{\partial\tilde{\psi}_h(\mathrm{r}_\Gamma,\mathrm{r}'_\Gamma)}{\partial \mathrm{n}'_\Gamma} q_{g'}(\mathrm{r}'_\Gamma) - \tilde{\psi}_h(\mathrm{r}_\Gamma,\mathrm{r}'_\Gamma)\frac{\partial q_{g'}(\mathrm{r}'_\Gamma)}{\partial \mathrm{n}'_\Gamma}\right] d\Gamma' \\ &\cong \sum_{j=1}^{I}\int_{-1}^{1}\left\{\frac{\partial\tilde{\psi}_h}{\partial \mathrm{n}'_\Gamma}\left[\mathrm{r}_{\Gamma,i},\mathrm{r}'_{\Gamma,j}+\tau\left(\mathrm{r}_{\Gamma,j+\frac{1}{2}}-\mathrm{r}_{\Gamma,j-\frac{1}{2}}\right)\right] q_{g',j}\right. \\ &\left.-\tilde{\psi}_h\left[\mathrm{r}_{\Gamma,i},\mathrm{r}'_{\Gamma,j}+\tau\left(\mathrm{r}_{\Gamma,j+\frac{1}{2}}-\mathrm{r}_{\Gamma,j-\frac{1}{2}}\right)\right] q'_{g',j}\right\}\frac{d_j}{2}d\tau. \end{aligned} \tag{53}$$

The integrals herewith appearing are obtained by application of a numerical integration formula, namely:

$$\int_{-1}^{1} f(\tau)d\tau \simeq \sum_{k=1}^{K}\omega_k f(\tau_k) \tag{54}$$

Table 1: Material data for the homogeneous core.

g	Σ_r^g	$\nu\Sigma_f^g$	D^g	$\Sigma_s^{g\to g+1}$	$\Sigma_s^{g\to g+2}$	χ^g
	$[\mathrm{cm}^{-1}]$	$[\mathrm{cm}^{-1}]$	[cm]	$[\mathrm{cm}^{-1}]$	$[\mathrm{cm}^{-1}]$	-
1	$0.3046E-01$	$0.1076E-01$	2.11	$0.2578E-01$	$0.5164E-03$	0.7737
2	$0.7060E-02$	$0.3309E-02$	1.29	$0.4705E-02$	–	0.2193
3	$0.6316E-02$	$0.4366E-02$	0.86	–	–	0.0070

where ω_k and τ_k are the standard quadrature weights and abscissae, respectively. In the present work a Gauss-Legendre formula is used.

At last the problem is cast into the following algebraic matrix-response form:

$$\sum_{g'=1}^{G}\sum_{j=1}^{I} M_{gg',ij}J^+_{g'j} = \sum_{g'=1}^{G}\sum_{j=1}^{I} N_{gg',ij}J^-_{g'j} + \sum_{g'=1}^{G}\sum_{j=1}^{I} K_{gg',ij}q_{g'j} + \sum_{g'=1}^{G}\sum_{j=1}^{I} L_{gg',ij}q'_{g'j}, \tag{55}$$

$$i = 1,2,\ldots,I, g = 1,2,\ldots,G,$$

where:

$$M_{gg',ij} = \frac{c(\mathrm{r})}{2}\delta_{i,j}\delta_{g,g'} + \frac{d_j}{2}\int_{-1}^{1}\tilde{J}^-_{gg'}\left[\mathrm{r}_{\Gamma,i}, \mathrm{r}'_{\Gamma,j} + \tau\left(\mathrm{r}_{\Gamma,j+\frac{1}{2}} - \mathrm{r}_{\Gamma,j-\frac{1}{2}}\right)\right]d\tau,$$

$$N_{gg',ij} = -\frac{c(\mathrm{r})}{2}\delta_{i,j}\delta_{g,g'} + \frac{d_j}{2}\int_{-1}^{1}\tilde{J}^+_{gg'}[\mathrm{r}_{\Gamma,i}, \mathrm{r}'_{\Gamma,j} + \tau\left(\mathrm{r}_{\Gamma,j+\frac{1}{2}} - \mathrm{r}_{\Gamma,j-\frac{1}{2}}\right)]d\tau,$$

$$K_{gg',ij} = -\sum_{h=1}^{G}\sigma_{gh}\frac{1}{4B_h^2}\sigma^*_{hg'}\left\{c(\mathrm{r})\delta_{i,j} + \frac{d_j}{2}\int_{-1}^{1}\frac{\partial\tilde{\psi}_h}{\partial\mathrm{n}'_\Gamma}[\mathrm{r}_{\Gamma,i}, \mathrm{r}'_{\Gamma,j} + \tau\left(\mathrm{r}_{\Gamma,j+\frac{1}{2}} - \mathrm{r}_{\Gamma,j-\frac{1}{2}}\right)]d\tau\right\},$$

$$L_{gg',ij} = \sum_{h=1}^{G}\sigma_{gh}\frac{1}{4B_h^2}\sigma^*_{hg'}\frac{d_j}{2}\int_{-1}^{1}\tilde{\psi}_h\left[\mathrm{r}_{\Gamma,i}, \mathrm{r}'_{\Gamma,j} + \tau\left(\mathrm{r}_{\Gamma,j+\frac{1}{2}} - \mathrm{r}_{\Gamma,j-\frac{1}{2}}\right)\right]d\tau. \tag{56}$$

The problem for the whole system where nodes are coupled is then solved by numerical iteration schemes.

6 Verification of numerical consistency and convergence of methods

It is worth going through a verification of the performance of various numerical approaches by comparison of results with highly accurate benchmark results that may be obtained directly by an analytical formula. Therefore a homogeneous rectangular system is now considered,

Table 2: Errors in the calculation of the effective multiplication factor for the homogeneous benchmark; the analytical value is $k = 0.90145$. Relative errors are expressed in pcm for the various models.

Nodes	FD	N	BEM 0 10 24	BEM 1 10 24	BEM 1 10 240	BEM 1 20 240
4	929	18	9070	494	495	498
8	235	1	2654	21	26	33
12	103	0	1283	9	3	5
16	57	0	787	14	9	0
20	37	0	554	16	10	2
24	25	0	426	17	11	2
28	18	0	349	18	11	2
32	14	0	299	18	12	2
36	11	0	264	18	12	2
40	8	0	239	18	12	3

Table 3: Cross sections for the reflector in the heterogeneous case.

g	Σ_r^g	D^g	$\Sigma_s^{g\to g+1}$	$\Sigma_s^{g\to g+2}$
	[cm^{-1}]	[cm]	[cm^{-1}]	[cm^{-1}]
1	$0.9667E-02$	2.52	$0.9506E-02$	$0.1270E-03$
2	$0.1508E-02$	1.56	$0.1385E-02$	–
3	$0.1407E-03$	1.00	–	–

Table 4: Results for the calculation of k for the reflected system.

Nodes	N	BEM 1 10 24	BEM 1 10 240	BEM 1 20 240
4	1.04923	1.04905	1.04914	1.04916
8	1.04924	1.04906	1.04921	1.04922
12	1.04924	1.04901	1.04921	1.04922
16	1.04924	1.04895	1.04921	1.04922
20	1.04924	1.04889	1.04920	1.04922
24	1.04924	1.04883	1.04919	1.04922
28	1.04924	1.04877	1.04919	1.04921
32	1.04924	1.04871	1.04918	1.04921
36	1.04924	1.04865	1.04918	1.04921
40	1.04924	1.04859	1.04917	1.04920

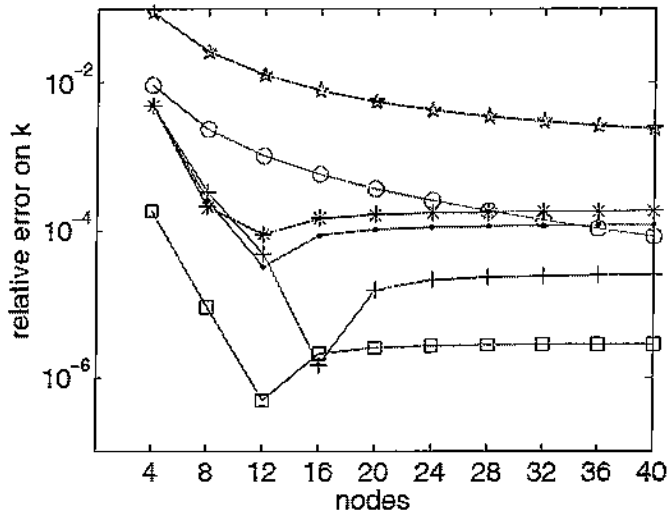

Figure 1: Convergence pattern for the calculation of the homogeneous system. FD (○); N (□); BEM 0 10 24 (⋆); BEM 1 10 24 (∗); BEM 1 10 240 (•); BEM 1 20 240 (+).

whose dimensions are 160 cm and 140 cm. The material data for a three-group model are reported in Table 1. A critical calculation is carried out and errors with respect to the analytical value of the effective multiplication constant are reported in Table 2. The various models are identified as follows: FD indicates the finite difference scheme, N is nodal, BEM $\alpha\beta\gamma$ denotes a distribution of order α for the source (0, constant, or 1, linear, in the present work), β the number of points used for the discretization of each edge and γ the order of the quadrature formula for integration. The number reported in the node column indicates the number of nodes assumed for each coordinate: hence the number of nodes covering the 2D domain increases as the square of the indicated number. The performance of the nodal method is quite remarkable, while good results are obtained by BEM only with a first-order approximation of the source distribution. Also, it is important to call the attention on the important role associated to the number of points used for the discretization of the boundary.

Furthermore, it is interesting to observe the convergence pattern for the methods studied, Fig. 1. While FD shows a monotonic behaviour, Nodal and some BEM methods are characterized by non-monotonic trends and reach a saturation. Such properties for the convergence of nodal methods are well-known to exist [12] and would deserve deeper investigation. They are connected to the assumption of the spatial distribution within the node, which, in general, may not be consistent with the physical model as described by the differential equations to be solved.

Some final considerations concerning the computational effort are in order. Considering Fig. 2, it is clear that to obtain relative errors below 10 pcm nodal and BEM are by far more effective.

A non-homogeneous system is also considered, to test the performance of the schemes in

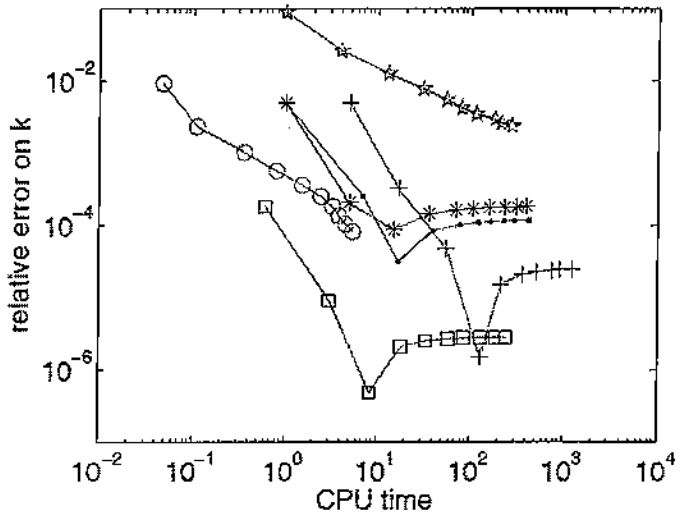

Figure 2: Relative errors vs. computational times for the homogeneous reactor calculation. Identification of curves as in previous figure.

the presence of a spatial interface. The symmetrical core is 180 cm wide and characterized by the data reported in Table 1. The data for the 90 cm thick reflector are specified in Table 3. The system is reflected only in the x-direction. The number of nodes herewith indicated refers to the discretization in the x-direction only, since along y only two nodes are used with zero-current on the boundary condition, to simulate an infinite medium. Results concerning k values are reported in Table 4.

7 Results for a realistic fast-spectrum configuration

A realistic fast-spectrum system is considered, with physical characteristics of the same type as the ones characterizing the ELSY project. The core is constituted by three regions, with increasing multiplicativities passing from the inner to the outermost regions. Lead is assumed for the coolant and the reflector. Cross sections are provided by spectrum and homogenization calculations carried out by the ENEA group participating to the ELSY project [13]. The sketch of the system and the nuclear data for the core regions and for the reflector are reported in Fig. 3 and Table 5.

- real reactor (3fuels + lead - two dimension with and without transverse buckling - nodal method assumed only) - graphs for flux and adjoint)

As already anticipated, adjoints may well serve in many interesting and useful applications in nuclear core analysis. Once the physical problem is cast into an algebraic form, the adjoint problem is easily constructed by taking the mathematical adjoint of the matrix operators appearing in the model. It is then possible to compute neutron importances that may be

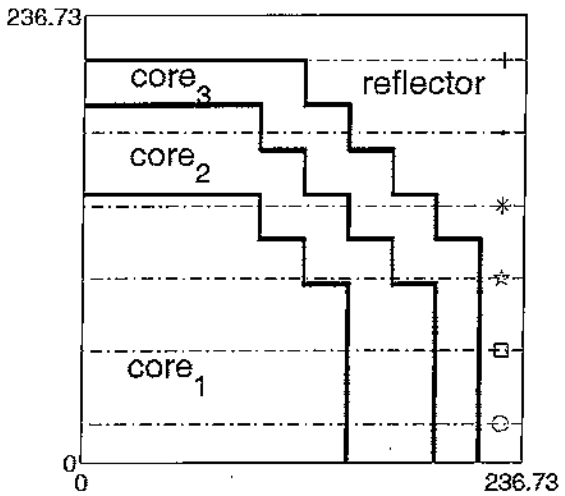

Figure 3: Geometrical configuration of the ELSY-like system.

used for sensitivity and perturbation analyses and for the construction of integral parameters for time-dependent calculations. The results of some such calculations are now presented in Figs. 4-9.

8 Conclusions and future developments

A neutronic module for multidimensional multigroup diffusion calculations is developed. Different discretization algorithms are implemented and tested. Some benchmark calculations allow to assess the consistency and applicability of various techniques. Nodal methods are shown to perform adequately for the simulation of fast spectrum systems, such as lead-cooled reactors. Realistic calculations are carried out for a system characterized by properties similar to the system adopted as the basis of the ELSY project.

As a future development, it is foreseen to couple the neutronic module developed in the frame of this work with a thermo-hydraulic code. This would allow to have a flexible and efficient computational tool for the assessment of the ELSY project and for parametric calculations aimed at the neutronic-thermal-hydraulic optimization.

A further future development will consider the extension of the computational tool to allow time-dependent evaluations within a quasi-static approach. To that end, the module can perform already adjoint calculations. The extension is to be done following the same philosophy as the one already employed for other recent applications [14].

Table 5: Material data for the ELSY-like reactor.

g	Σ_r^g	$\nu\Sigma_f^g$	D^g	$\Sigma_s^{g\to g+1}$	$\Sigma_s^{g\to g+2}$	χ^g
	[cm^{-1}]	[cm^{-1}]	[cm]	[cm^{-1}]	[cm^{-1}]	-
CORE$_1$						
1	$0.3303E-01$	$0.1076E-01$	2.11	$0.2578E-01$	$0.5164E-03$	0.7737
2	$0.8638E-02$	$0.3309E-02$	1.29	$0.47052E-02$	–	0.2193
3	$0.7369E-02$	$0.4366E-02$	0.86	–	–	0.0070
CORE$_2$						
1	$0.3306E-01$	$0.1146E-01$	2.11	$0.2562E-01$	$0.5135E-03$	0.7737
2	$0.8651E-02$	$0.3698E-02$	1.30	$0.4576E-02$	–	0.2194
3	$0.7460E-02$	$0.4766E-02$	0.86	–	–	0.0069
CORE$_3$						
1	$0.3314E-01$	$0.1267E-01$	2.11	$0.2531E-01$	$0.5071E-03$	0.7735
2	$0.8711E-02$	$0.4551E-02$	1.31	$0.4324E-02$	–	0.2195
3	$0.7675E-02$	$0.5629E-02$	0.87	–	–	0.0070
REFLECTOR						
1	$0.1274E-01$	–	2.52	$0.9506E-02$	$0.1270E-03$	–
2	$0.3413E-02$	–	1.56	$0.1385E-02$	–	–
3	$0.1358E-02$	–	1.00	–	–	–

9 Acknowledgments

The work is performed with the support of the ELSY project (VI European Framework Program). The Authors are grateful to XXX and XXX of ENEA-Bologna for providing the cross section data utilized for the simulations. One of the Authors (H. S.) acknowledges the support received by the Zhong Guo program and by the Asia Link Project "An EU-China Campus for Energy and Environment" for making available the opportunity of a PhD program on Energy Engineering at Politecnico di Torino.

References

[1] L. Cinotti, G. Locatelli, H. Aït Abderrahim, S. Monti, G. Benamati, K. Tucek, D. Struwe, A. Orden, G. Corsini, D. Le Carpentier, "The ELSY Project," in *Proceedings of the International Conference on the Physics of Reactors "Nuclear Power: A Sustainable Resource" (PHYSOR 08)*, Interlaken, Switzerland, September 2008.

[2] S. Langenbuch, W. Werner, W. Maurer, "Coarse-mesh flux-expansion method for the analysis of space-time effects in large light water reactor cores," *Nuclear Science and Engineering*, **63**, 437–456 (1977).

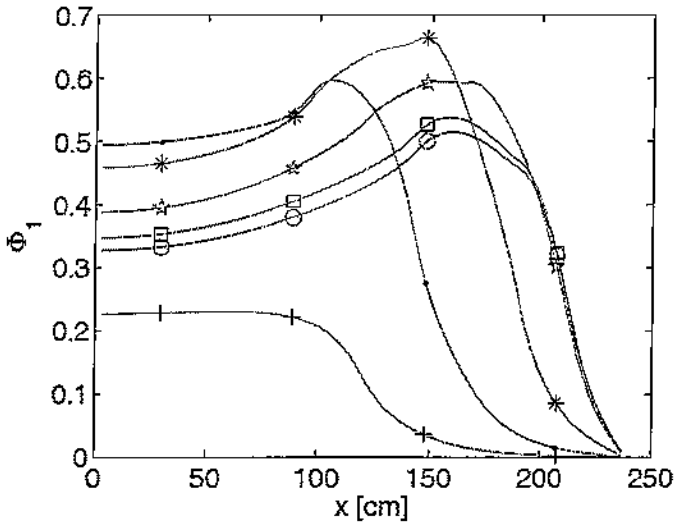

Figure 4: Graphs of the first-group (high energy) fluxes. Symbols on curves identify fluxes plotted along the transverses bearing the same symbol indicated in Fig. 3.

[3] M. Maiani, B. Montagnini, "A boundary element - response matrix method for the multigroup neutron diffusion equations," *Annals of Nuclear Energy*, **26**, 1341–1369 (1999).

[4] M. Maiani, B. Montagnini, "A Galerkin approach to the boundary element-response matrix method for the multigroup neutron diffusion equations" *Annals of Nuclear Energy*, **31**, 1447-1475 (2004).

[5] S. Dulla, E.H. Mund, P. Ravetto, "The quasi-static method revisited" *Progress in Nuclear Energy*, **50**, 908-920 (2008).

[6] E.E. Lewis, W.F. Miller, Jr., *Computational methods of neutron transport*, Wiley, New York (1984).

[7] P. Camiciola, D. Cundari, B. Montagnini, "A coarse-mesh method for 1-D reactor kinetics", *Annals of Nuclear Energy*, **13**, 629-636 (1986).

[8] B. Montagnini, P. Sorapeira, C. Trentavizi, M. Sumini, D.M. Zardini, "A well-balanced coarse-mesh flux expansion method", *Annals of Nuclear Energy*, **21**, 45-53 (1994).

[9] C.A. Brebbia, J. Dominguez, *Boundary elements: an introductory course*, Computational Mechanics Publications, Southampton (1992).

[10] R. Ciolini, G.G.M. Coppa, B. Montagnini, P. Ravetto, "Simplified P_N and A_N methods in neutron transport", *Progress in nuclear energy*, **40**, 237-264 (2002).

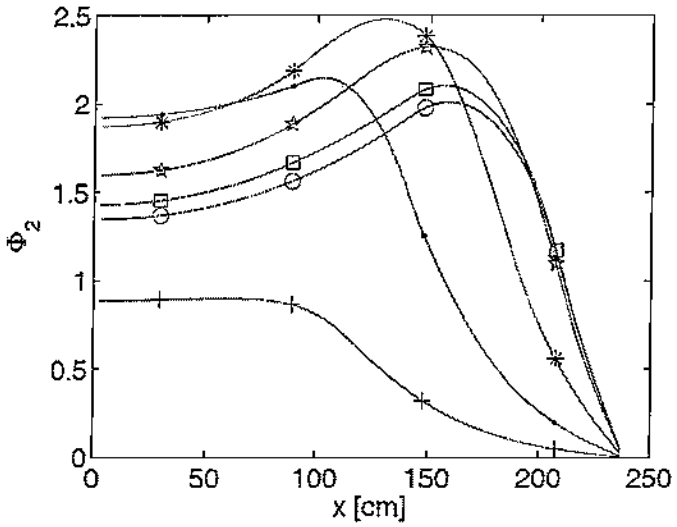

Figure 5: Graphs of the second group (intermediate energy) fluxes.

[11] S. Canepa, R. Van Geemert, D. Porsch, S. Dulla, P. Ravetto, "A response matrix formulation of multidimensional transport problems," in *Proceedings of the International Conference on the Physics of Reactors "Nuclear Power: A Sustainable Resource" (PHYSOR 08)*, Interlaken, Switzerland, September 2008.

[12] Zhang Shaohong, Li Ziyong, Y. A. Chao, "A Theoretical Study on A Convergence Problem of Nodal Methods," in *Proceedings of the International Conference on the Physics of Reactors (PHYSOR 06)*, Vancouver, Canada, September 2006.

[13] ENEA, private communication (2008).

[14] P. Picca, E.H. Mund, S. Dulla, P. Ravetto, G. Marleau, "A quasi-static transport module using the DRAGON code," in *Proceedings of the International Conference on the Physics of Reactors "Nuclear Power: A Sustainable Resource" (PHYSOR 08)*, Interlaken, Switzerland, September 2008.

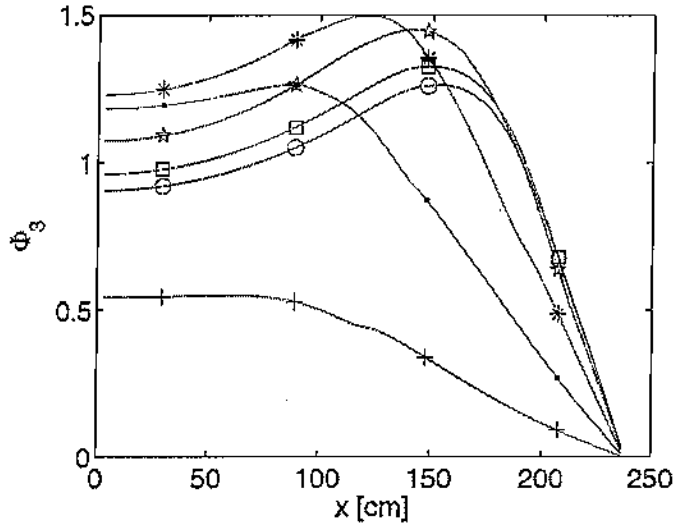

Figure 6: Graphs of the third group (low energy) fluxes.

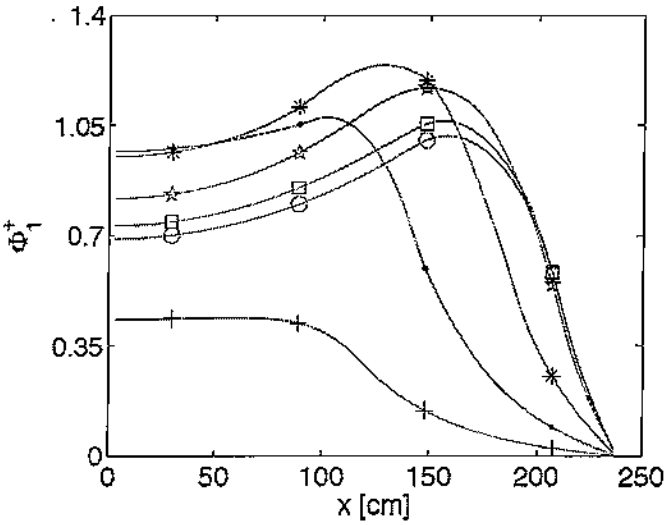

Figure 7: Graphs of the neutron importance for the first group.

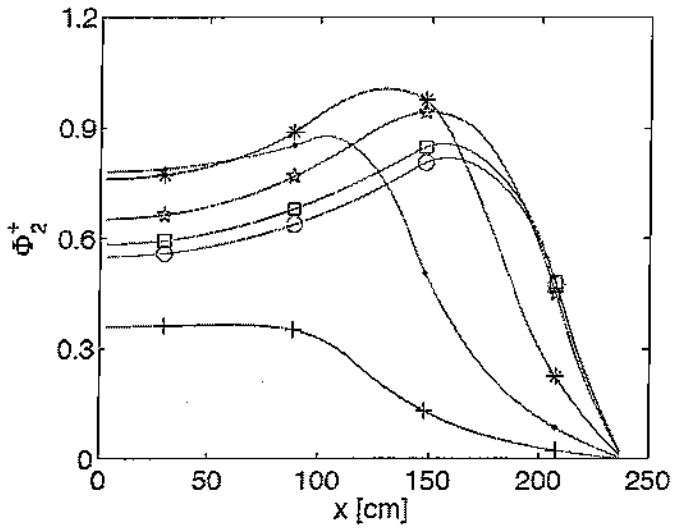

Figure 8: Graphs of the neutron importance for the second group.

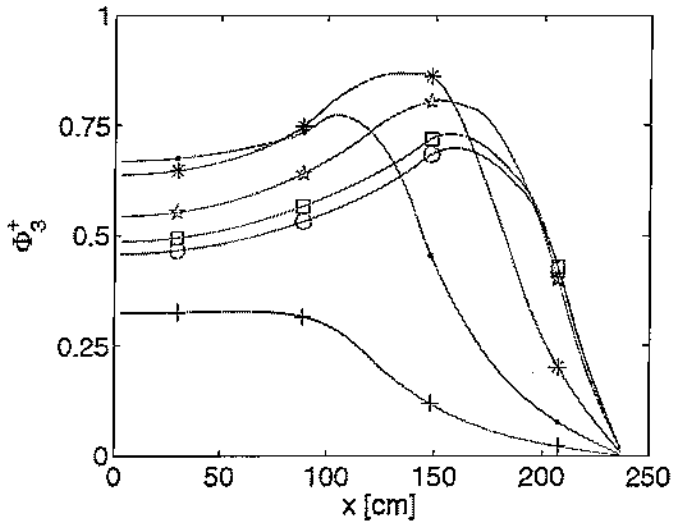

Figure 9: Graphs of the neutron importance for the third group.